Comparison of Choroidal Vascularity Markers on Optical Coherence Tomography Using Two-Image Binarization Techniques

Xin Wei,[1] Shozo Sonoda,[2] Chitaranjan Mishra,[3] Neha Khandelwal,[4] Ramasamy Kim,[3] Taiji Sakamoto,[2] and Rupesh Agrawal[4,5]

[1]Khoo Teck Puat Hospital, Singapore
[2]Department of Ophthalmology, Kagoshima University Graduate School of Medical and Dental Sciences, Kagoshima, Japan
[3]Aravind Eye Hospital, Madurai, India
[4]National Healthcare Group Eye Institute, Tan Tock Seng Hospital, Singapore
[5]Moorfields Eye Hospital, NHS Foundation Trust, London, United Kingdom

Correspondence: Rupesh Agrawal, National Healthcare Group Eye Institute, Tan Tock Seng Hospital, Singapore 308433; rupeshttsh@gmail.com.

Submitted: August 1, 2017
Accepted: December 26, 2017

Citation: Wei X, Sonoda S, Mishra C, et al. Comparison of choroidal vascularity markers on optical coherence tomography using two-image binarization techniques. *Invest Ophthalmol Vis Sci*. 2018;59:1206–1211. https://doi.org/10.1167/iovs.17-22720

Purpose. To compare the agreement between optical coherence tomography (OCT)-based choroidal vascularity markers measured by two previously reported image binarization techniques.

Methods. Spectral-domain OCT using enhanced-depth imaging was performed in 100 eyes from 52 normal subjects. Choroidal images were binarized to luminal area and stromal area using two different algorithms. Choroidal vascularity marker was defined as the ratio of luminal area to total choroidal area and they were termed "luminal/choroidal area ratio (L/C ratio)" and "choroidal vascularity index (CVI)" per the algorithm. The agreement between choroidal vascularity markers measured by the two techniques was compared using intraclass correlation coefficient (ICC) and Bland-Altman analysis.

Results. The mean values of choroidal vascularity markers were 70.12% (range, 56.76%–78.55%) for CVI and 67.44% (range, 51.09%–81.31%) for L/C ratio. Low level of absolute agreement between the two binarization techniques was reflected by an adjusted ICC of 0.353 using linear mixed model with age, sex, and spherical equivalent as covariates.

Conclusions. There was discrepancy between measurements of choroidal vascularity using two commonly adopted image binarization techniques. It remained unclear what was the true choroidal vascularity and which binarization algorithm was more accurate. Future studies with enhanced image quality and improved image analysis algorithm are required to decipher the ground truth for choroidal vascularity.

Keywords: choroid, optical coherence tomography, image binarization, choroidal vascularity

The choroid is a richly vascularized and pigmented tissue, consisting of blood vessels as well as stromal tissue, including extracellular matrix and melanocytes.[1] It has the highest blood flow per body weight among all tissues in the body.[2] Choroid is responsible for the vascular supply to the outer retina, RPE, and possibly part of the optic nerve.[3–5] Dysfunction of the choroid is implicated in common ocular diseases such as age-related macular degeneration[6,7] and diabetic retinopathy.[8] Recent literature also suggest that choroidal structural changes are associated with many systemic diseases.[9]

Various methods have been attempted to understand the changes in choroid in disease states, such as histologic evaluation[10]; indocyanine green angiography (ICGA)[11]; ultrasonography[12]; and optical coherence tomography (OCT).[13–15]

OCT offers an in vivo noninvasive quantitative assessment of choroidal structure, especially with the advent of enhanced-depth imaging (EDI) technique.[16] Choroidal thickness (CT) is the most commonly used OCT derived marker of choroidal structure.[17] However, the use of CT has an inherent disadvantage of inability to differentiate changes in the choroidal vascular versus stromal area due to structural heterogeneity of choroid.

Recently development of OCT image binarization techniques has allowed for differentiation and quantification of choroidal vascular and stromal areas separately.[18,19] This has led to the creation of a novel structural marker for choroidal vascularity, which is the ratio of vascular (or luminal) area to total choroidal area. It was termed "choroidal vascularity index (CVI)" by Agrawal et al.[19] or "luminal/choroidal area ratio (L/C ratio)" by Sonoda et al.[18] This new marker of choroidal vascularity has been investigated in normal physiologic conditions[18,20–23] and also validated as a useful tool in various ocular diseases.[19,24–36]

Differences exist in the image binarization algorithms for the calculation of CVI and L/C ratio.[20] Although they are measuring the same entity, there is no direct head-to-head comparison between the two. There is also no gold standard that they can be compared against. In this study, we aim to investigate the agreement between CVI and L/C ratio measured by two-image binarization techniques in a group of healthy subjects.

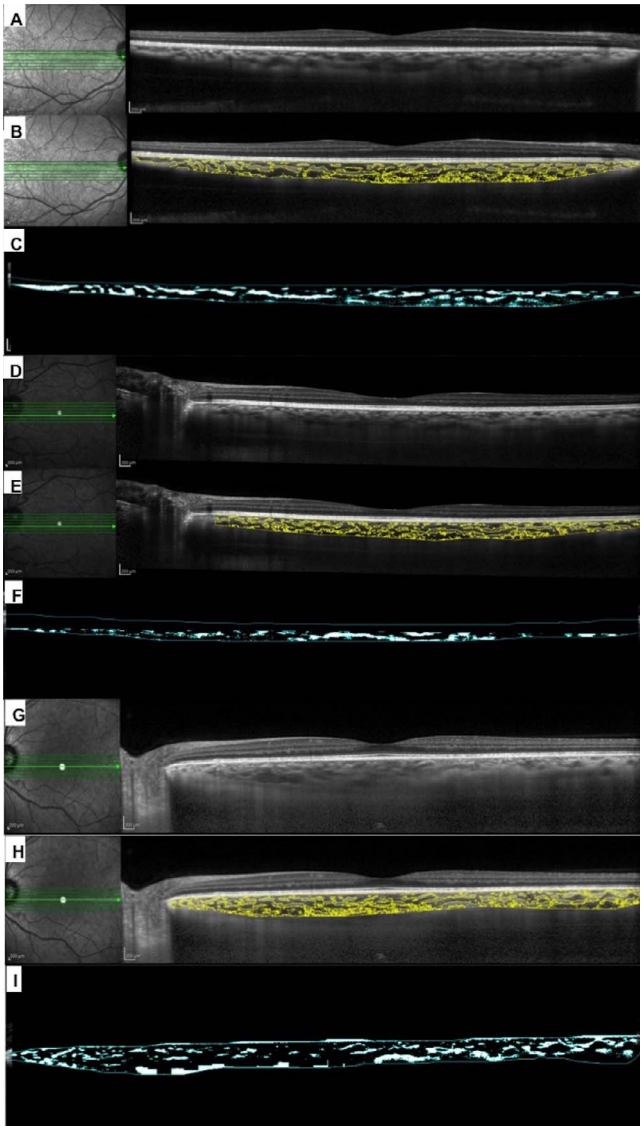

FIGURE 1. Examples of OCT images before and after binarization. (**A**, **D**, **E**) Original spectral-domain OCT images. (**B**, **E**, **H**) OCT images after binarization using technique proposed by Agrawal et al.[19] (**C**, **F**, **I**) OCT images after binarization using technique proposed by Sonoda et al.[18] (**A–C**) One subject in which choroidal vascularity index (CVI) is similar to luminal/ choroidal ratio (L/C ratio). (**D–F**) One subject in which CVI is smaller than L/C ratio. (**G–I**) One subject in which CVI is larger than L/C ratio.

METHODOLOGY

We performed image analysis of EDI spectral domain OCT in healthy subjects. Study participants were recruited from a tertiary eye center in India between August and December 2016. They were included if best corrected visual acuity was 6/6 in both eyes and media was clear. Subjects with any systemic illnesses or any ocular pathology were excluded. Prior approval was obtained from the Institutional Review Board and informed consent was obtained from each subject. This study adhered to the tenets of Declaration of Helsinki.

Measurement of Ocular Factors

All subjects were evaluated by certified ophthalmologists and refracted by certified optometrists. Best corrected visual acuity was measured by Snellen chart. Spherical equivalent (SE) was calculated as the sum of the spherical power and half of the cylindrical power.

Image Acquisition

All subjects underwent EDI-OCT scans using a commercial device (Spectralis; Heidelberg Engineering, Vista, CA, USA). The macular region was scanned using a 7-horizontal line scan ($30° \times 5°$) centered on the fovea, with 100 frames averaged in each B-scan. Each scan was 8.9 mm in length and spaced 240 μm apart from each other.

Image Analysis

The raster scan passing through the fovea was selected for analysis. Binarization was performed separately using techniques proposed by Sonoda et al.[18] and Agrawal et al.[19] Detailed algorithms for both techniques were described previously. Both techniques were carried out with ImageJ (version 1.47; provided in the public domain by the National Institutes of Health, Bethesda, MD, USA; https://imagej.nih.gov/ij/).[37]

In the technique proposed by Sonoda et al.,[18] choroidal segmentation was performed before binarization by manual plotting of the total choroidal area (TCA) extending from RPE/Bruch's membrane complex to the choroid-sclera interface. Subsequently, average brightness of the choroidal luminal area (LA) was calculated as the mean reflectivity of three randomly selected choroidal vessels with lumens larger than 100 μm. By setting this value as the minimal brightness of the image, the OCT scan was converted to an 8-bit image. The 8-bit image was then binarized using a Niblack auto local threshold tool. Lastly, the binarized image was converted to a red, green, blue image to allow selection of choroidal LA (the area with dark pixels) by the color threshold tool. The ratio of choroidal LA to TCA (L/C ratio) was calculated automatically by the software.

In the technique proposed by Agrawal et al.,[19] a few modifications were made. The OCT scan was directly converted to 8-bit images using ImageJ default setting. Then the 8-bit image was binarized using Niblack auto local threshold tool in the same manner. This was followed by choroidal segmentation by manual plotting of choroidal inner and outer border, which highlighted the TCA. The final steps of choroidal LA selection was the same as technique of Sonoda et al.[18] Size of LA and TCA were calculated by the software and CVI was computed by dividing LA by TCA.

Examples of OCT images before and after binarization using both techniques was illustrated in Figure 1. The representative images also demonstrated the discrepancies in L/C ratio and CVI in three subjects (Fig. 1).

Statistical Analysis

The degree of agreement between choroidal vascularity indices calculated by the two techniques was evaluated using intraclass correlation coefficient (ICC) and visualization of the agreement was obtained using Bland-Altman analysis. ICC was expressed in terms of absolute agreement and obtained using two-way mixed model. Crude or unadjusted ICC between the two techniques was obtained using actual values of CVI and L/C ratio, while adjusted ICC was obtained using a linear mixed model due to its ability to deal with correlated data for bilateral eye involvement. Adjustment was performed using age, sex, and SE as covariates. All statistical analyses were performed using statistical software (SPSS version 20.0; IBM Corp. Armonk, NY, USA) and statistical significance was evaluated at 5% level.

Investigative Ophthalmology & Visual Science

Table 1. Descriptive Statistics of Demographics and CV of Study Subjects and the Agreement Between CVI and L/C Ratio Using Unadjusted and Adjusted ICC

	Mean ± SD	Range	Unadjusted ICC (95% CI)	Adjusted ICC (95% CI)
Age, y	38.13 ± 12.64	19 to 65		
Female sex, %	55.77			
Refractive error, diopters	−0.11 ± 0.66	−2.875 to +1.25		
CVI, %	70.12 ± 3.87	56.76 to 78.55	0.372 (0.074 to 0.576)*	0.353 (−0.202 to 0.667)†
L/C ratio, %	67.44 ± 5.14	51.09 to 81.31		

* $P = 0.004$.
† $P < 0.001$.

Results

We included 100 eyes from 52 patients in this study. Both eyes were eligible in 48 patients and one eye was eligible in four patients. The mean age was 38.13 years (range, 19–65). There were 23 males and 29 females in the study (Table 1). The mean value for CVI was 70.12% (range: 56.76%–78.55%, SD: 3.87%), while the mean value for L/C ratio was 67.44% (range: 51.06–81.31%, SD: 5.14%; Table 1).

Two-way mixed, average measure ICC was used to assess absolute agreement between CVI and L/C ratio. ICC was used instead of Pearson's correlation coefficient as ICC gives the closeness between the two measurements, while correlation provides only the linearity of two measurements. The crude or unadjusted ICC obtained was 0.372 (95% confidence interval [CI]: 0.074–0.576; *P* value: 0.004), which indicated low level of absolute agreement between CVI or L/C ratio (Table 1). Subsequently, linear mixed model (LMM) was used to calculate the adjusted values for CVI and L/C ratio using age, sex, and SE as covariates. Since measurements were taken on both eyes for one subject, LMM considered these measurements as repeated and correlated values. Table 2 provided the β coefficients of covariates for CVI and L/C ratio. Age and SE were statistically significantly correlated with CVI ($P = 0.029$ and $P < 0.001$ respectively), while sex was significantly correlated with L/C ratio ($P = 0.020$). The adjusted ICC using LMM was 0.353 (95% CI: –0.202 to 0.667; $P < 0.001$; Table 1), which still suggested poor absolute agreement between CVI and L/C ratio.

Visualization of agreement was obtained using Bland-Altman plots before (Fig. 2A) and after (Fig. 2B) adjustment with covariates (Fig. 2). Before adjustment, the limits of agreement were wider (–8.12 to 13.47) compared to those after agreement (–0.79 to 6.17). Despite that, both Bland-Altman plots and ICC value indicated poor agreement between the two techniques.

Discussion

Binarization of OCT choroidal images has led to the creation of new tools to assess choroidal structure in vivo. In contrary to the current OCT-based markers (i.e., CT and choroidal volume), which measure overall structural changes, these biomarkers for choroidal vascularity (i.e., CVI and L/C ratio), encompass changes in both vascular and stromal components of the choroid.

Performance of choroidal vascularity markers were studied in both healthy and diseased eyes and it was evident these new markers were valuable and robust. CVI but not CT, was shown to be independent from systemic and ocular factors such as age, axial length, intraocular pressure, or systolic blood pressure in a large study involving 345 normal subjects.[20] In eyes from diabetic patients and eyes with exudative AMD, there were decreased CVI with no significant change in CT.[26,28,29] CVI was also shown to provide additional information to CT in terms of longitudinal choroidal structural changes in diseases such as panuveitis[20]; Vogt-Koyanagi-Harada (VKH) disease[25]; central serous chorioretinopathy (CSCR)[24]; and myopic choroidal neovascularization.[27] Changes in L/C ratio or a similar index called L/S ratio (ratio of choroidal luminal area to stromal area) were investigated and found to yield valuable information in normal physiologic conditions including diurnal variation[22] and dynamic exercise[23] as well as in a number of ocular diseases including exudative AMD[21]; polypoidal choroidal vasculopathy (PCV)[34]; CSCR[32,33]; VKH disease[30,31]; and retinitis pigmentosa.[36]

In this study, we compared the agreement between markers of choroidal vascularity (CVI and L/C ratio) measured by two-image binarization techniques and significant differences were found between the two measurements. CVI was shown to be higher by 2% to 3% compared to L/C ratio. In addition, L/C ratio was statistically different between male and female, whereas CVI was influenced by age and refractive error. As both techniques derived a statistically different index for vascularity in the choroid, the effect of the confounding variables could be different. CVI seemed to be more equivocal for male and female, whereas L/C ratio was robust for differences in refractive error and age.

The assumption that dark pixels in OCT images represented choroidal luminal area and that light pixels represented choroidal stromal area was the foundation of analysis in both techniques. To date, there was no direct and definitive

Table 2. Association of CVI and L/C Ratio With Age, Sex, and SE

	CVI				L/C Ratio			
		95% CI for β				95% CI for β		
Factors	β	Lower Limit	Upper Limit	*P* Value	β	Lower Limit	Upper Limit	*P* Value
Age	−0.083	−0.158	−0.009	0.029*	−0.070	−0.165	0.025	0.144
Female sex	−0.549	−2.433	1.335	0.560	−2.881	−5.286	−0.477	0.020*
Refractive error, SE	2.552	1.290	3.814	<0.001*	0.781	−0.930	2.492	0.365

β, regression coefficient.
* *P* values < 0.05 represent significance level.

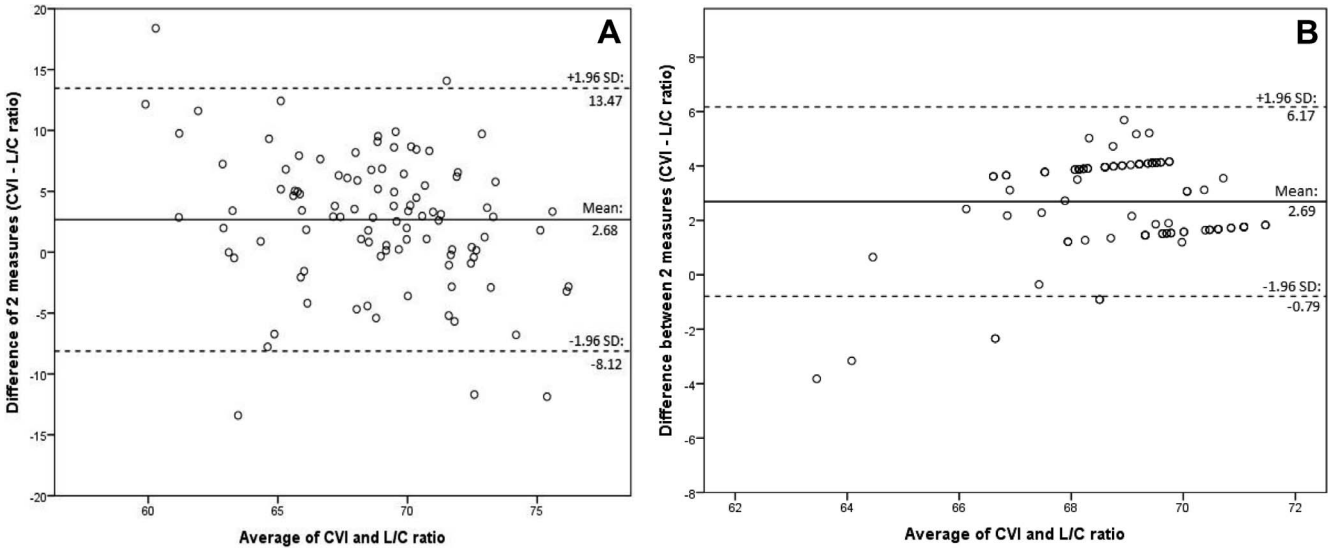

FIGURE 2. Agreement between CVI and L/C ratio using Bland-Altman plot. (**A**) Illustrates the plot using unadjusted agreement. (**B**) Illustrates the plot with adjusted agreement for the covariates and bilateral eyes.

evidence to prove this assumption. However, earlier published studies and empirical observations strongly suggested that the assumption was true.[13,38] On the other hand, there were also evidence suggesting light-scattering pattern on OCT was affected by choroidal melanin pigments and this could complicate the interpretation of light and dark pixels.[39,40] In their previous publications, authors of both techniques have compared binarized images to the original OCT images and showed that dark area corresponded to lumens of choroidal vessels.[18,19] Both authors have also demonstrated high intragrader and intergrader reliability of their measurements in previous reports.[18,19]

Discrepancy in CVI and L/C ratio could be explained by the differences in methodology. First, in the technique used by Agrawal et al.,[19] image binarization using Niblack auto local thresholding was performed prior to manual plotting of choroidal inner and outer border. In contrast, image binarization was carried out after identification of choroidal borders in the algorithm used by Sonoda et al.[18] Differences in the determination of choroidal borders might result in different measurement of TCA, which was the denominator in the calculation of choroidal vascularity markers. Second, Agrawal et al.[19] used ImageJ default setting for the conversion of original OCT image to 8-bit image and omitted the step used by Sonoda et al.[18] which set a threshold with preselection of three large vessel lumens. This could translate into a higher minimum brightness value used as the threshold in Sonoda et al.[18] technique and hence a smaller measurement of LA, which was the numerator in the CVI or L/C ratio calculation.

The key step in the measurement of choroidal vascularity is image analysis and thresholding, which are intrinsically subjective unless supported by additional evidence. Niblack auto local threshold strategy is the technique of choice used in both methods discussed in this paper primarily because of their effectiveness in isolating vascular structures.[18,41] Image binarization, and indeed thresholding of any kind, is specific to the object of interest in the image. There are several well-accepted thresholding techniques based on image histograms; clustering; entropy; object attributes; spatial methods; local adaptive methods; rank filters; region adjacency graph methods; partial derivative equation methods (level-sets); Hessian analyses; and the recently popular supervised deep neural networks. The most commonly used methods utilize the properties of the image histogram to identify regions of interest. These methods include Otsu, Yen, Li, Renyi entropy, Intermodes, Sauvola, and Bernsen. Each of these methods makes certain assumptions about the data. For example, the Intermodes method assumes that the histogram is bimodal, which makes images with histograms having extremely unequal peaks or a broad and flat valley unsuitable for this method.[42] Otsu's threshold clustering algorithm finds the threshold that minimizes the intraclass variance of background and foreground pixels.[43] Recently Hessian analysis and texture mapping have been shown to be very effective in isolating vasculature from images of the fundus.[44] These methods utilize a deep understanding of the image properties such as the need to remove speckle noise and local curvature values to give optimal segmentation. In cases of fundus images, the ground-truth of the location of vascular structure is readily verified, unlike in OCT images. Deep neural networks have become very powerful in recent times. Systems such as Segnet[45] and U-net[46] are very powerful at identifying regions of interest. The major drawback of neural-networks is that they have to be trained with known ground-truth parameters. Currently the actual vascular status is not known in OCT images, which is not ideal for the application of neural networks. So far the gold standard for the methods of image binarization is still lacking. Further research with evidence to support the isolation of true vascular structures is required for a gold standard to be developed.

A higher CVI value compared to L/C ratio could be the result of larger choroidal LA or smaller TCA or a combination of both. We were also unable to comment on accuracy of the two techniques due to the lack of a gold standard in measuring choroidal vascularity. In future studies, we aim to compare image datasets of normal eyes with different disease phenotypes using the two different techniques to explore those disease datasets as possible silver standards to compare the effectiveness of the two software. These were the limitations of our study. The strengths of our study were a large sample size, homogenous ethnicity, and correction for factors such as age, sex, and refractive error so that effect of confounding factors could be minimized.

In conclusion, we report poor agreement between choroidal vascularity markers measured by two OCT choroidal image binarization techniques. It remains unclear what was the true

choroidal vascularity and which binarization technique was more accurate. Further studies to address these questions are warranted and will likely require improved image analysis algorithm as well as advancement in OCT with enhanced image quality, better signal-to-noise ratio and higher contrast.

Acknowledgments

Disclosure: **X. Wei**, None; **S. Sonoda**, None; **C. Mishra**, None; **N. Khandelwal**, None; **R. Kim**, None; **T. Sakamoto**, None; **R. Agrawal**, None

References

1. Nickla DL, Wallman J. The multifunctional choroid. *Prog Retin Eye Res*. 2010;29:144–168.
2. Alm A, Bill A. Ocular and optic nerve blood flow at normal and increased intraocular pressures in monkeys (*Macaca irus*): a study with radioactively labelled microspheres including flow determinations in brain and some other tissues. *Exp Eye Res*. 1973;15:15–29.
3. Castro-Correia J. Understanding the choroid. *Int Ophthalmol*. 1995;19:135–147.
4. Kur J, Newman EA, Chan-Ling T. Cellular and physiological mechanisms underlying blood flow regulation in the retina and choroid in health and disease. *Prog Retin Eye Res*. 2012; 31:377–406.
5. Hayreh SS. The blood supply of the optic nerve head and the evaluation of it - myth and reality. *Prog Retin Eye Res*. 2001; 20:563–593.
6. Ma L, Tang SM, Rong SS, et al. Association of PEDF polymorphisms with age-related macular degeneration and polypoidal choroidal vasculopathy: a systematic review and meta-analysis. *Sci Rep*. 2015;5:9497.
7. Matsuoka M, Ogata N, Otsuji T, Nishimura T, Takahashi K, Matsumura M. Expression of pigment epithelium derived factor and vascular endothelial growth factor in choroidal neovascular membranes and polypoidal choroidal vasculopathy. *Br J Ophthalmol*. 2004;88:809–815.
8. Melancia D, Vicente A, Cunha JP, Abegao Pinto L, Ferreira J. Diabetic choroidopathy: a review of the current literature. *Graefes Arch Clin Exp Ophthalmol*. 2016;254:1453–1461.
9. Tan KA, Gupta P, Agarwal A, et al. State of science: Choroidal thickness and systemic health. *Surv Ophthalmol*. 2016;61: 566–581.
10. Fryczkowski AW, Sato SE, Hodes BL. Changes in the diabetic choroidal vasculature: scanning electron microscopy findings. *Ann Ophthalmol*. 1988;20:299–305.
11. Guyer DR, Puliafito CA, Mones JM, Friedman E, Chang W, Verdooner SR. Digital indocyanine-green angiography in chorioretinal disorders. *Ophthalmology*. 1992;99:287–291.
12. Coleman DJ, Lizzi FL. In vivo choroidal thickness measurement. *Am J Ophthalmol*. 1979;88:369–375.
13. Branchini LA, Adhi M, Regatieri CV, et al. Analysis of choroidal morphologic features and vasculature in healthy eyes using spectral-domain optical coherence tomography. *Ophthalmology*. 2013;120:1901–1908.
14. Adhi M, Brewer E, Waheed NK, Duker JS. Analysis of morphological features and vascular layers of choroid in diabetic retinopathy using spectral-domain optical coherence tomography. *JAMA Ophthalmol*. 2013;131:1267–1274.
15. Mrejen S, Spaide RF. Optical coherence tomography: imaging of the choroid and beyond. *Surv Ophthalmol*. 2013;58:387–429.
16. Spaide RF, Koizumi H, Pozzoni MC. Enhanced depth imaging spectral-domain optical coherence tomography. *Am J Ophthalmol*. 2008;146:496–500.
17. Laviers H, Zambarakji H. Enhanced depth imaging-OCT of the choroid: a review of the current literature. *Graefes Arch Clin Exp Ophthalmol*. 2014;252:1871–1883.
18. Sonoda S, Sakamoto T, Yamashita T, et al. Luminal and stromal areas of choroid determined by binarization method of optical coherence tomographic images. *Am J Ophthalmol*. 2015;159: 1123–1131.e1.
19. Agrawal R, Gupta P, Tan KA, Cheung CM, Wong TY, Cheng CY. Choroidal vascularity index as a measure of vascular status of the choroid: Measurements in healthy eyes from a population-based study. *Sci Rep*. 2016;6:21090.
20. Agrawal R, Salman M, Tan KA, et al. Choroidal vascularity index (CVI)–a novel optical coherence tomography parameter for monitoring patients with panuveitis? *PLoS One*. 2016; 11:e0146344.
21. Sonoda S, Sakamoto T, Yamashita T, et al. Choroidal structure in normal eyes and after photodynamic therapy determined by binarization of optical coherence tomographic images. *Invest Ophthalmol Vis Sci*. 2014;55:3893–3899.
22. Kinoshita T, Mitamura Y, Shinomiya K, et al. Diurnal variations in luminal and stromal areas of choroid in normal eyes. *Br J Ophthalmol*. 2017;101:360–364.
23. Kinoshita T, Mori J, Okuda N, et al. Effects of exercise on the structure and circulation of choroid in normal eyes. *PLoS One*. 2016;11:e0168336.
24. Agrawal R, Chhablani J, Tan KA, Shah S, Sarvaiya C, Banker A. Choroidal vascularity index in central serous chorioretinopathy. *Retina*. 2016;36:1646–1651.
25. Agrawal R, Li LK, Nakhate V, Khandelwal N, Mahendradas P. Choroidal vascularity index in Vogt-Koyanagi-Harada disease: an EDI-OCT derived tool for monitoring disease progression. *Trans Vis Sci Tech*. 2016;5(4):7.
26. Koh LH, Agrawal R, Khandelwal N, Sai Charan L, Chhablani J. Choroidal vascular changes in age-related macular degeneration. *Acta Ophthalmol*. 2017;95:e597–e601.
27. Ng WY, Ting DS, Agrawal R, et al. Choroidal structural changes in myopic choroidal neovascularization after treatment with antivascular endothelial growth factor over 1 year. *Invest Ophthalmol Vis Sci*. 2016;57:4933–4939.
28. Tan KA, Laude A, Yip V, Loo E, Wong EP, Agrawal R. Choroidal vascularity index - a novel optical coherence tomography parameter for disease monitoring in diabetes mellitus? *Acta Ophthalmol*. 2016;94:E612–E616.
29. Wei X, Ting DS, Ng WY, Khandelwal N, Agrawal R, Cheung CM. Choroidal vascularity index: a novel optical coherence tomography based parameter in patients with exudative age-related macular degeneration. *Retina*. 2016;37:1120–1125.
30. Egawa M, Mitamura Y, Akaiwa K, et al. Changes of choroidal structure after corticosteroid treatment in eyes with Vogt-Koyanagi-Harada disease. *Br J Ophthalmol*. 2016;100:1646–1650.
31. Kawano H, Sonoda S, Yamashita T, Maruko I, Iida T, Sakamoto T. Relative changes in luminal and stromal areas of choroid determined by binarization of EDI-OCT images in eyes with Vogt-Koyanagi-Harada disease after treatment. *Graefes Arch Clin Exp Ophthalmol*. 2016;254:421–426.
32. Kinoshita T, Mitamura Y, Mori T, et al. Changes in choroidal structures in eyes with chronic central serous chorioretinopathy after half-dose photodynamic therapy. *PLoS One*. 2016; 11:e0163104.
33. Sonoda S, Sakamoto T, Kuroiwa N, et al. Structural changes of inner and outer choroid in central serous chorioretinopathy determined by optical coherence tomography. *PLoS One*. 2016;11:e0157190.
34. Daizumoto E, Mitamura Y, Sano H, et al. Changes of choroidal structure after intravitreal aflibercept therapy for polypoidal choroidal vasculopathy. *Br J Ophthalmol*. 2017;101:56–61.

Investigative Ophthalmology & Visual Science

35. Izumi T, Koizumi H, Maruko I, et al. Structural analyses of choroid after half-dose verteporfin photodynamic therapy for central serous chorioretinopathy. *Br J Ophthalmol*. 2017;101:433–437.
36. Kawano H, Sonoda S, Saito S, Terasaki H, Sakamoto T. Choroidal structure altered by degeneration of retina in eyes with retinitis pigmentosa. *Retina*. 2017;37:2175–2182.
37. Schneider CA, Rasband WS, Eliceiri KW. NIH Image to ImageJ: 25 years of image analysis. *Nat Methods*. 2012;9:671–675.
38. Sohrab M, Wu K, Fawzi AA. A pilot study of morphometric analysis of choroidal vasculature in vivo, using en face optical coherence tomography. *PLoS One*. 2012;7:e48631.
39. Pellegrini M, Shields CL, Arepalli S, Shields JA. Choroidal melanocytosis evaluation with enhanced depth imaging optical coherence tomography. *Ophthalmology*. 2014;121:257–261.
40. Yiu G, Vuong VS, Oltjen S, et al. Effect of uveal melanocytes on choroidal morphology in rhesus macaques and humans on enhanced-depth imaging optical coherence tomography. *Invest Ophthalmol Vis Sci*. 2016;57:5764–5771.
41. Niblack W. *An Introduction to Digital Image Processing*. Eaglewood Cliffs, NJ: Prentice Hall; 1986.
42. Prewitt JM, Mendelsohn ML. The analysis of cell images. *Ann N Y Acad Sci*. 1966;128:1035–1053.
43. Otsu N. A threshold selection method from gray-level histograms. *IEEE Trans Syst Man Cybern Syst*. 1979;9:62–66.
44. Yin X, Ng BWH, He J, Zhang Y, Abbott D. Accurate image analysis of the retina using hessian matrix and binarisation of thresholded entropy with application of texture mapping. *PLoS One*. 2014;9:e95943.
45. Badrinarayanan V, Kendall A, Cipolla R. SegNet: a deep convolutional encoder-decoder architecture for image segmentation. *IEEE Trans Pattern Anal Mach Intell*. 2017;39:2481–2495.
46. Ronneberger O, Fischer P, Brox T. U-net: convolutional networks for biomedical image segmentation. In: Navab N, Hornegger J, Wells W, Frangi A, eds. *Medical Image Computing and Computer-Assisted Intervention. Lecture Notes in Computer Science*. Vol. 9351. Cham: Springer, Cham; 2015.

Investigative Ophthalmology & Visual Science